·Article·
Advances in Polar Science
doi: 10.3724/SP.J.1085.2013.00265
December 2013 Vol. 24 No. 4: 265-272

Near-surface structure and energy characteristics of the Antarctic Circumpolar Current

GAO Libao[1, 2*], YU Weidong[1], WANG Haiyuan[1] & LIU Yanliang[1]

[1] Center for Ocean and Climate Research, First Institute of Oceanography, Qingdao 266061, China;
[2] College of Physical and Environmental Oceanography, Ocean University of China, Qingdao 266100, China

Received 8 June 2013; accepted 11 October 2013

Abstract Historical surface drifter observations collected from the Southern Ocean are used to study the near-surface structure, variability, and energy characteristics of the Antarctic Circumpolar Current (ACC). A strong, nearly zonal ACC combined with complex fronts dominates the circulation system in the Southern Ocean. Standard variance ellipses indicate that both the Agulhas Return Current and the East Australian Warm Current are stable supplements of the near-surface ACC, and that the anticyclonic gyre formed by the Brazil warm current and the Malvinas cold current is stable throughout the year. During austral winter, the current velocity increases because of the enhanced westerly wind. Aroused by the meridional motion of the ACC, the meridional velocity shows greater instability characteristics than the zonal velocity does over the core current. Additionally, the ACC exhibits an eastward declining trend in the core current velocity from southern Africa. The characteristics of the ACC are also argued from the perspective of energy. The energy distribution suggests that the mean kinetic energy (MKE), eddy kinetic energy (EKE), and $\sqrt{\mathrm{EKE}}$ are strong over the core currents of the ACC. However, in contrast, EKE/MKE suggests there is much less (more) eddy dissipation in regions with strong (weak) energy distribution. Both meridional and zonal energy variations are studied to illustrate additional details of the ACC energy characteristics. Generally, all the energy forms except EKE/MKE present west-east reducing trends, which coincide with the velocity statistics. Eddy dissipation has a much greater effect on MKE in the northern part of the Southern Ocean.

Keywords **mean structure, energy characteristic, ACC**

Citation: Gao L B, Yu W D, Wang H Y, et al. Near-surface structure and energy characteristics of the Antarctic Circumpolar Current. Adv Polar Sci, 2013, 24:265-272, doi: 10.3724/SP.J.1085.2013.00265

1 Introduction

The Antarctic Circumpolar Current (ACC) is the most important current in the Southern Ocean, and it is the only current that flows around the entire globe. It flows eastwards through the southern portions of the Atlantic, Indian, and Pacific oceans, providing the primary means by which water, heat, and salt are exchanged between them. Therefore, variations in the transport of the ACC may influence the Earth's climate over a range of timescales[1].

The current's boundaries are defined generally by zonal variations in specific water properties of the Southern Ocean[2]. Variations in these properties have been used to classify regions, the edges of which are defined by fronts marking rapid changes in water properties that occur over short distances. North of the ACC is the Subtropical Convergence or Subtropical Front (STF), usually found between 35°S and 45°S, where both the average sea surface temperature (SST) changes from about 12℃ to 8℃ and the salinity decreases from over 34.9 to 34.6 or less.

Maps of the gradient of sea surface height and SST reveal that the ACC comprises multiple jets or frontal filaments[3]. Three fronts and three zones south of the STF associated with the ACC are, from north to south: the Subantarctic Zone (SAZ), the Subantarctic Front (SAF), the Polar Frontal Zone, the Polar Front (PF), the Antarctic Zone, and the Southern ACC Front.

The energy characteristics and regional mean circulation of the ACC have been studied in previous papers. For

* Corresponding author (email: gaolb@fio.org.cn)

instance, Piola et al. compiled a data set of 280 drifting buoys and prepared maps of mean surface velocity, kinetic energy, and momentum flux between 20°S and 68°S, providing an initial evaluation of those fields in the Southern Hemisphere[4]. Associated energy and momentum transfer processes in the Southern Ocean are assessed by comparing model statistics with altimeter observations[5]. Baroclinic transport variability of the ACC near 140°E is estimated from six occupations of a repeat section occupied as part of the World Ocean Circulation Experiment. It is found that the mean top-to-bottom volume transport is around 147 Sv, relative to a deep reference level consistent with water mass properties and float trajectories. The location and transport of the main fronts of the ACC are relatively steady[6]. Assireu et al. used data from 15 drifters to provide detailed aspects of the surface circulation and kinetic energy along the Brazil Current between 24°S and 37°S[7]. More recently, the southwestern Atlantic mean surface circulation and its associated variability and energetics have been studied through the analysis of 13 years' data from surface drifters. The analysis of the kinetic energy conversion term suggests the presence of barotropic instabilities along the Brazil Current. Over most of the Brazil Current region, the kinetic energy conversion term points from the mean to the EKE[8].

Following the recent increase in their spatial and temporal coverage, surface drifters provide one of the best sources of information on the velocity field for estimating mean currents and energetics in remote oceanic areas[9]. Given that most previous studies have focused either on the ACC characteristics deduced from satellite observations or on the regional associated energetics deduced from drifter data, we intend to extend the understanding of the mean structure and energy characteristics of ACC over the entire Southern Ocean by analyzing historical drifter data. The remainder of the paper is organized as follows. Section 1 describes the data and methodology we used. Section 2 presents the mean structure and variability of the ACC deduced from drifter data. Section 3 describes the ACC characteristics from energy perspective and Section 4 presents a summary of the major results.

2 Data and methods

Four data sets were used to extract the features of the ACC. The quality-control surface drifter data, obtained from the Global Drifter Program Drifter Data Assembly Center (http://www.aoml.noaa.gov/phod/dac/dacdata.html), was the primary data used in this study for the structure and energy analysis. The freely-drifting surface buoys were attached to drogues centered at 15-m depth and their trajectory data were collected by the Argos satellite system. Data used in this study, which covers a period of 1986–2013 were optimally interpolated to uniform six-hour interval trajectories[10]. The Tropical Rainfall Measuring Mission (TRMM)'s Microwave Imager is a passive microwave sensor designed to provide quantitative rainfall information over a wide swath under the TRMM satellite[11]. It provided us with high spatial resolution (0.25°×0.25°) SST data from 1997, which helped us realize the details of the main fronts in the Southern Ocean. The wind speed data used in this study are the annual mean climatology wind product from the National Centers for Environmental Prediction, China. The 1993–2002 mean surface geostrophic velocity was calculated from the mean dynamic ocean surface topography[12].

First of all, we reticulated the surface drifter data into a grid with spatial resolution about 1°×1°[13]. This grid size was chosen to give a reasonable depiction of the major ocean circulation features considering the Lagrangian time scale and length scale[8]. Following previous studies[4-5,7-10,13-14], the Euler velocity was estimated as the Reynolds average of the Lagrangian velocities in every bin. Finally, the kinetic energy distributions as well as the mean structure were produced to reveal the characteristics of the ACC. The related expressions are as follows:

$$\mathrm{MKE} = \frac{1}{2}(\overline{u}^2 + \overline{v}^2) \text{ and } \mathrm{EKE} = \frac{1}{2}(u'u' + v'v'), \quad (1)$$

where MKE and EKE represent the mean kinetic energy and eddy kinetic energy, respectively, $\overline{u}$ and $\overline{v}$ are the temporal mean of the Lagrangian velocity components within a six-hour interval, and u' and v' are the instantaneous deviation of Lagrangian velocity components[9,14].

3 Mean structure and variability of the ACC

Historical surface drifter observations from the Southern Ocean were collected to study the mean structure and variability of the ACC. Figure 1a shows that almost all of the bins were covered by more than 50 samples north of 60°S and that this number even exceeded 500 in most of the region north of 50°S. In contrast, the surface drifter observations near the Antarctic region were very sparse because of the blocking influence of sea ice. This means that we cannot capture the characteristics of the entire ACC, but can continue with the analysis of the basic characteristics of the core surface currents of the ACC.

A strong, nearly zonal ACC combined with complex fronts dominates the circulation system in the Southern Ocean. Climatological SST (annual mean from 1997–2012) gradient was used to describe the location and intensity of the fronts. Most of the high SST gradient values are located in the SAZ, which is defined as the region between the STF and SAF. It is clear from Figure 1b that the maximum SST gradient of over 3.5℃·(100 km)$^{-1}$ appears in the Agulhas Return Current region of the southwest Indian Ocean, followed by the next largest value (over 2℃·(100 km)$^{-1}$) in the region of the Brazil-Malvinas Confluence Zone.

The standard variance ellipses show variability of one standard deviation of the vectors about their mean. It is a useful way to plot the variability of both the magnitude and direction of vectors. Note that the ellipse is not necessarily oriented along the vector direction, but that it is rotated to the principal components of the variability. As shown in Figure 1c, the main currents in this region are described

accurately, especially in the zonal direction, in that most of the major axes of the standard variation ellipses are oriented in the north-south direction. This implies that the meridional velocity shows greater instability characteristics than the zonal velocity on the core current does, which is mostly aroused by the meridional motion of the ACC.

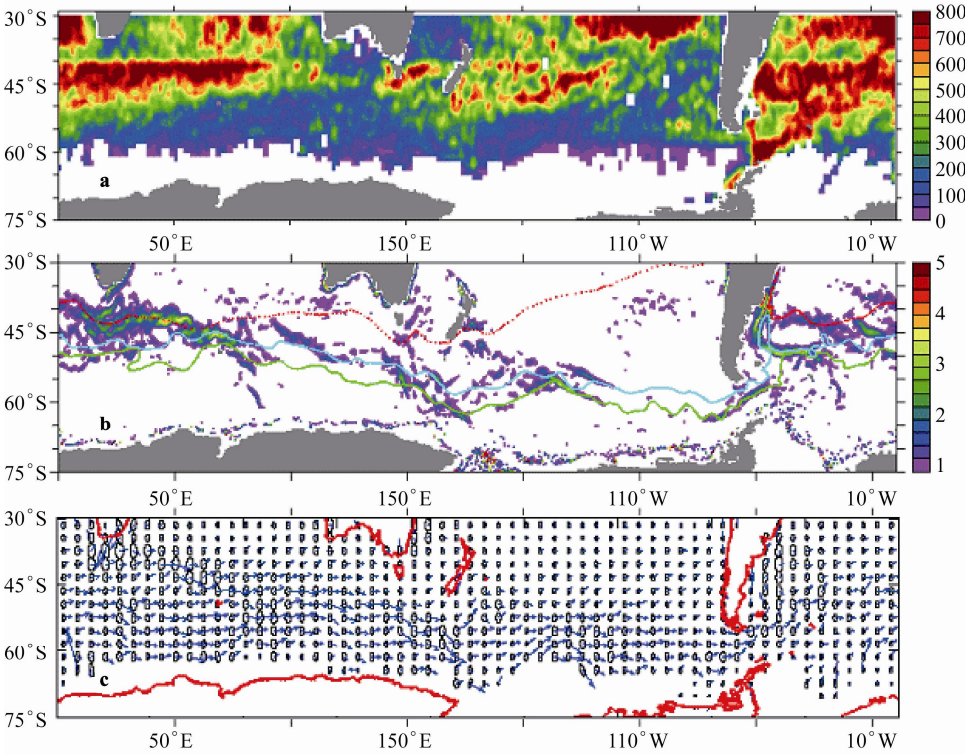

Figure 1 Historical Argos sample quantity in each bin (1°×1°) (**a**); SST gradient (shading, unit: ℃·(100 km)$^{-1}$) and main fronts in the southern ocean (red, STF; blue, SAF; green, PF) (**b**); standard variance ellipses and sea surface current. The fronts' positions are from Orsi et al.[15] (**c**).

Both the Agulhas Return Current and the East Australian Warm Current are stable supplements of the ACC, and the anticyclonic gyre formed by the Brazil warm current and the Malvinas cold current is stable throughout the year (Figure 2). The annual cycle of ACC velocity bears a strong resemblance to the annual cycle of wind speed (Figure 3). The current velocity is minimum (23.5 cm·s^{-1}) in February, corresponding to the lowest value of wind speed (3.7 m·s^{-1}). During the austral winter, the current velocity increases significantly (maximum is about 31 cm·s^{-1}) because of the enhanced westerly wind (maximum is about 5 m·s^{-1}). Additionally, the ACC exhibits an eastward decline trend in the core current velocity from the southern Africa (Table 1). The maximum mean velocities appear in the southwest Indian Ocean and exceed 42 cm·s^{-1}, whereas the minimum values are near 16 cm·s^{-1}.

Velocity component variations along the meridional and zonal sections of the austral summer and winter seasons are shown in Figure 4. The U component of the austral winter is 2–8 cm·s^{-1} larger than that during the austral summer along both the meridional and zonal sections (Figures 4a and 4c), correlating with the findings shown in Figure 2. The eastward declining trend of the ACC core current velocity, shown in Table 1, can also be identified in Figure 4c. Compared with the U component, the V component variation is much more complex (Figure 4b and 4d). The V component during the austral winter, south of 53°S and north of 37°S, is still larger than that during the austral summer, but the condition is reversed in the region between 37°S–53°S (Figure 4b). Additionally, extreme peaks around the region of 60°W–70°W are illustrated in Figure 4c and 4d. These are caused by the strong zonal current and western boundary current near the Drake Passage.

As can be seen from Figure 5, the surface geostrophic current is the main component of the surface current in the Southern Ocean in that they present similar magnitudes and directions. Therefore, it can be presumed that the energy characteristics from both the geostrophic aspect and the drifter aspect are largely similar.

4 Energy characteristic analysis of the ACC

In the following, we discuss the characteristics of the ACC from the perspective of energy. Eddy processes play two important roles in the MKE balance: kinetic energy conversion and kinetic energy redistribution[16]. The EKE, MKE, EKE/MKE, and $\sqrt{\text{EKE}}$ of the ACC are shown in Figure 6. The energy distribution suggests both the EKE and MKE

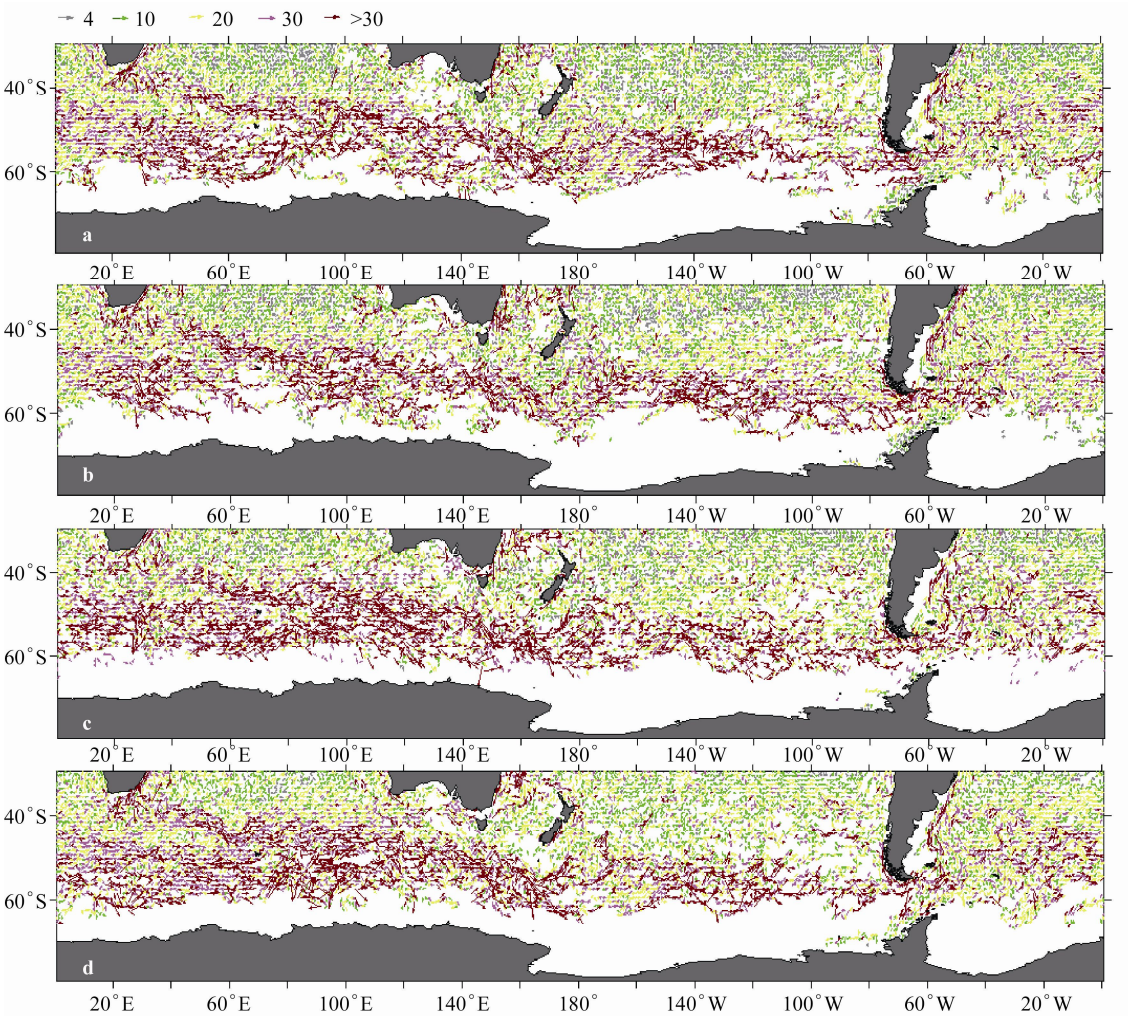

Figure 2 Seasonal sea surface current in the Southern Ocean (unit: cm·s^{-1}). **a**, SON; **b**, DJF; **c**, MAM; **d**, JJA.

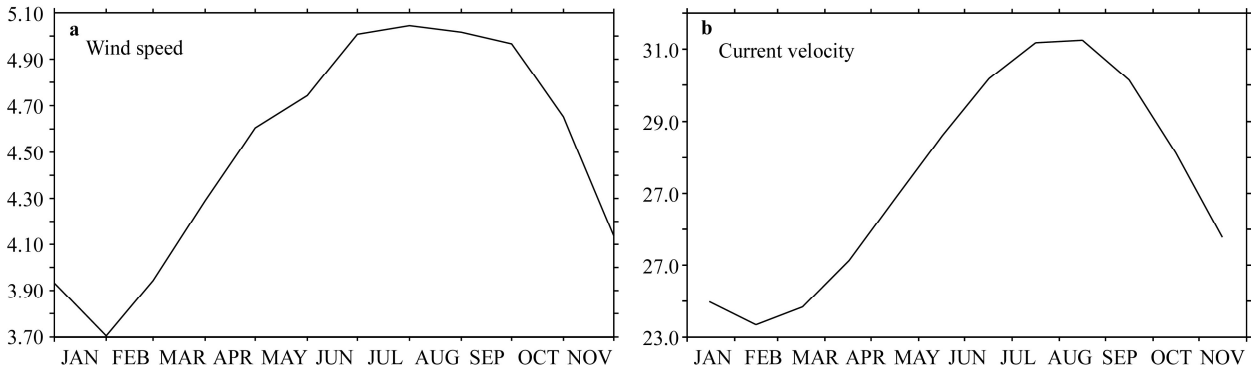

Figure 3 Annual cycles of wind speed and surface current in the Southern Ocean (35°S–65°S, 180°W–180°E). Wind speed (**a**, unit: m·s^{-1}); surface current velocity (**b**, only calculated for velocities greater than 20, unit: cm·s^{-1}).

Table 1 Zonal variations of the ACC velocity

Regions	35°S–65°S 20°E–40°E	35°S–65°S 70°E–90°E	35°S–65°S 130°E–150°E	35°S–65°S 160°W–140°W	35°S–65°S 90°W–70°W	35°S–65°S 30°W–10°W
Velocity/(cm·s^{-1})	44	42	36	34	30	16

are clearly strong over the core currents of the ACC. The maximum values of EKE of over 300 cm^2·s^{-2} appear in both the Agulhas Return Current region and the Brazil-Malvinas Confluence Zone (Figure 6a), which is much more similar

to the maximum SST gradient pattern, as shown in Figure 1b. This region is one of the most energetic regions of the world's oceans[8,17-18]. In contrast, the MKE represents a similar pattern, but the value of its amplitude is twice that of the EKE (Figure 6b).

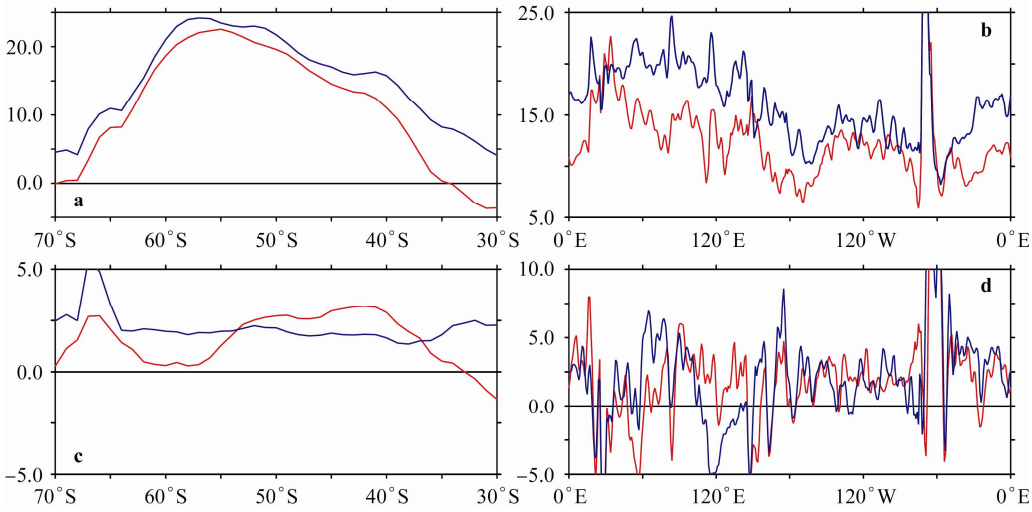

Figure 4 U component (upper level) and V component (lower level) variations of meridional (left panel) and zonal (right panel) sections in the Southern Ocean (observed from Argos, unit: cm·s^{-1}, red lines: mean values of DJF season; blue lines: mean values of JJA season).

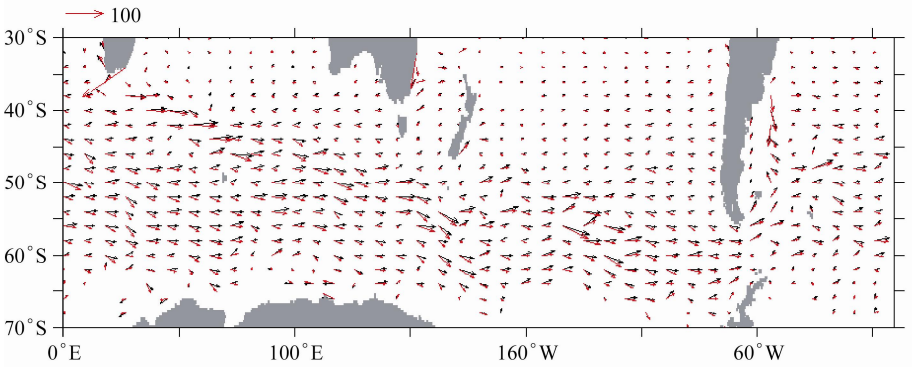

Figure 5 Surface current climatology derived from drifters (black) and 1993–2002 mean surface geostrophic current (red) in the Southern Ocean (unit: cm·s^{-1}).

The ratio between EKE and MKE can be recognized as an approximate indicator for barotropic instability[19]. It is worth noticing that the ratio between EKE and MKE is quite low (high) over (off) the core current region (Figure 6c). In other words, the low ratio values indicate that most of the main currents are dominated by mean flow rather than by shorter eddy fluctuations. Conversely, over most of the region away from the main current cores, the available potential energy in the ocean is depicted as being largely in the form of EKE. For example, over the core current region, eddy dissipation consumes less than 40% MKE, whereas more than 80% MKE is consumed by eddy dissipation away from the core current region. The value of $\sqrt{\text{EKE}}$ is comparable with the current velocity, which clearly shows the intensity distribution of velocity fluctuation. As shown in Figure 6d, almost all of the ACC core regions are associated with strong velocity fluctuations, as in the results shown in Figure 1c. This point agrees well with the findings of previous studies. Southern Ocean observations from surface drifters[20], current meters[21], and altimetry, all show high levels of eddy energy, particularly in the western boundary currents and major fronts of the ACC.

To illustrate additional details of the ACC energy characteristics, we introduce plots of the energy variations of the meridional and zonal sections in the Southern Ocean (Figure 7). The left-hand panels of Figure 7 show the meridional mean variations of energy. It is clear that EKE, MKE, and $\sqrt{\text{EKE}}$ show quite similar meridional trends in all the associated oceans. For instance, EKE, MKE, and $\sqrt{\text{EKE}}$ reach their peaks simultaneously around 55°S–60°S. Among all of the associated oceans, energy values of the Indian Ocean are the largest, whereas the smallest values appear in the Atlantic Ocean (Pacific Ocean) in the southern (northern) part of the Southern Ocean. In contrast with the one-peak phase in the other oceans, the Atlantic Ocean has double peaks around 47°S and 57°S (Figures 7a, 7b, and

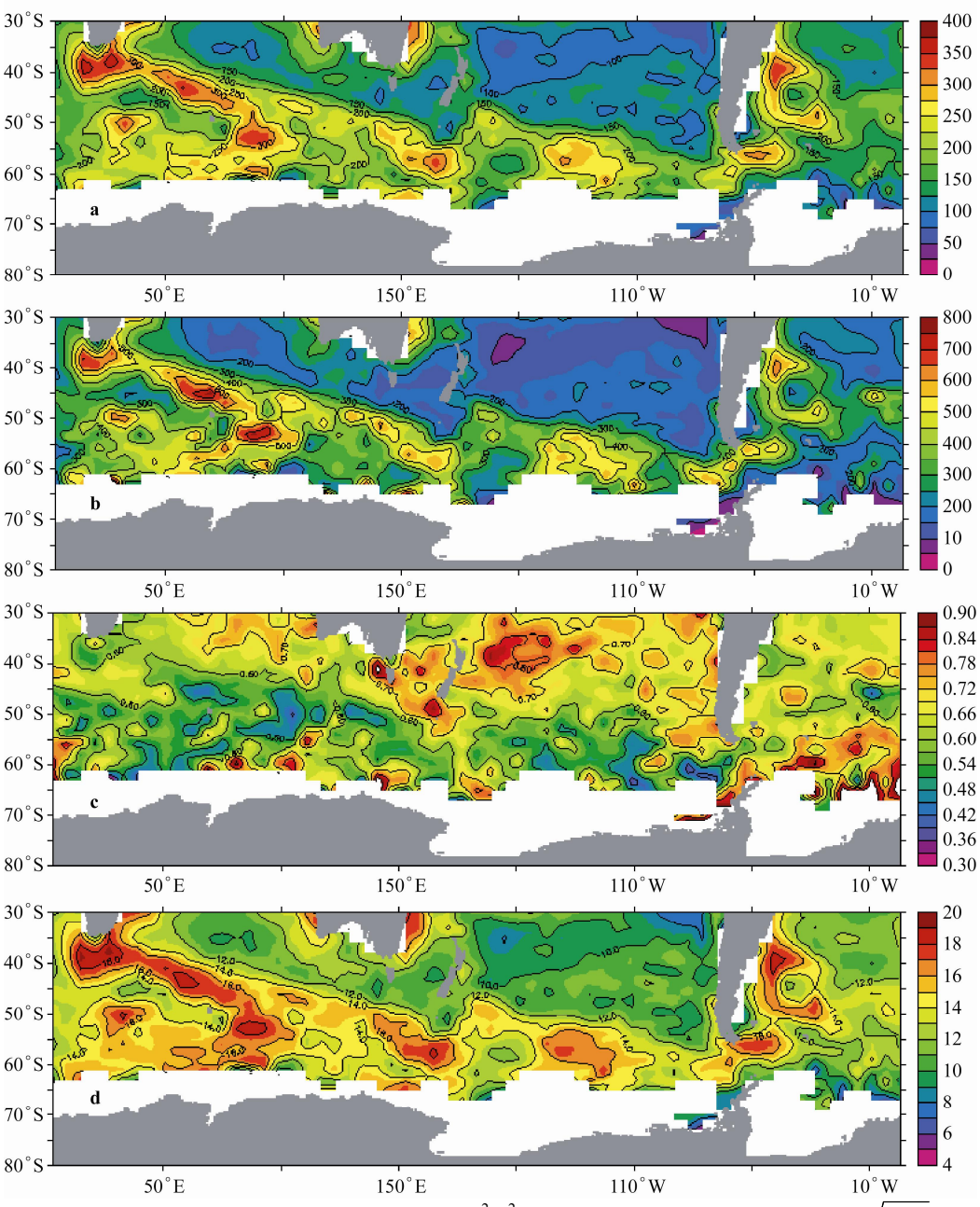

Figure 6 Energy distribution in the Southern Ocean (unit: $cm^2 \cdot s^{-2}$) . **a**, EKE; **b**, MKE; **c**, EKE/MKE; **d**, $\sqrt{EKE}$ (unit: $cm \cdot s^{-1}$).

7d). Compared with EKE, MKE, and $\sqrt{EKE}$, EKE/MKE is just the opposite, there is much less (more) eddy dissipation in regions with strong (weak) energy distribution (Figure 7c). The right-hand panels of Figure 7 show the zonal mean variations of energy. Generally, all the energy forms except EKE/MKE present west–east reducing trends, which coincide with the velocity statistics in Table 1. There is sharp contrast between the northern (30°S–45°S) and southern (45°S–60°S) parts of the Southern Ocean; EKE, MKE, and $\sqrt{EKE}$ are stronger in southern parts compared with the north (Figures 7e, 7f, and 7h). However, the situation for EKE/MKE is reversed (Figure 7g). This indicates that eddy dissipation has a much greater effect on MKE in the northern part of the Southern Ocean.

5 Summary

Historical surface drifter observations from the Southern Ocean were collected to study the mean structure, variability, energy characteristics of the ACC. The main results are summarized below.

(1) Surface drifter observations are sufficient for the analysis of near-surface structure and variability of the ACC. A strong, nearly zonal ACC combined with complex fronts dominates the circulation system in the Southern Ocean. The maximum SST gradient values appear mainly in the Agulhas Return Current region and the Brazil–Malvinas Confluence Zone.

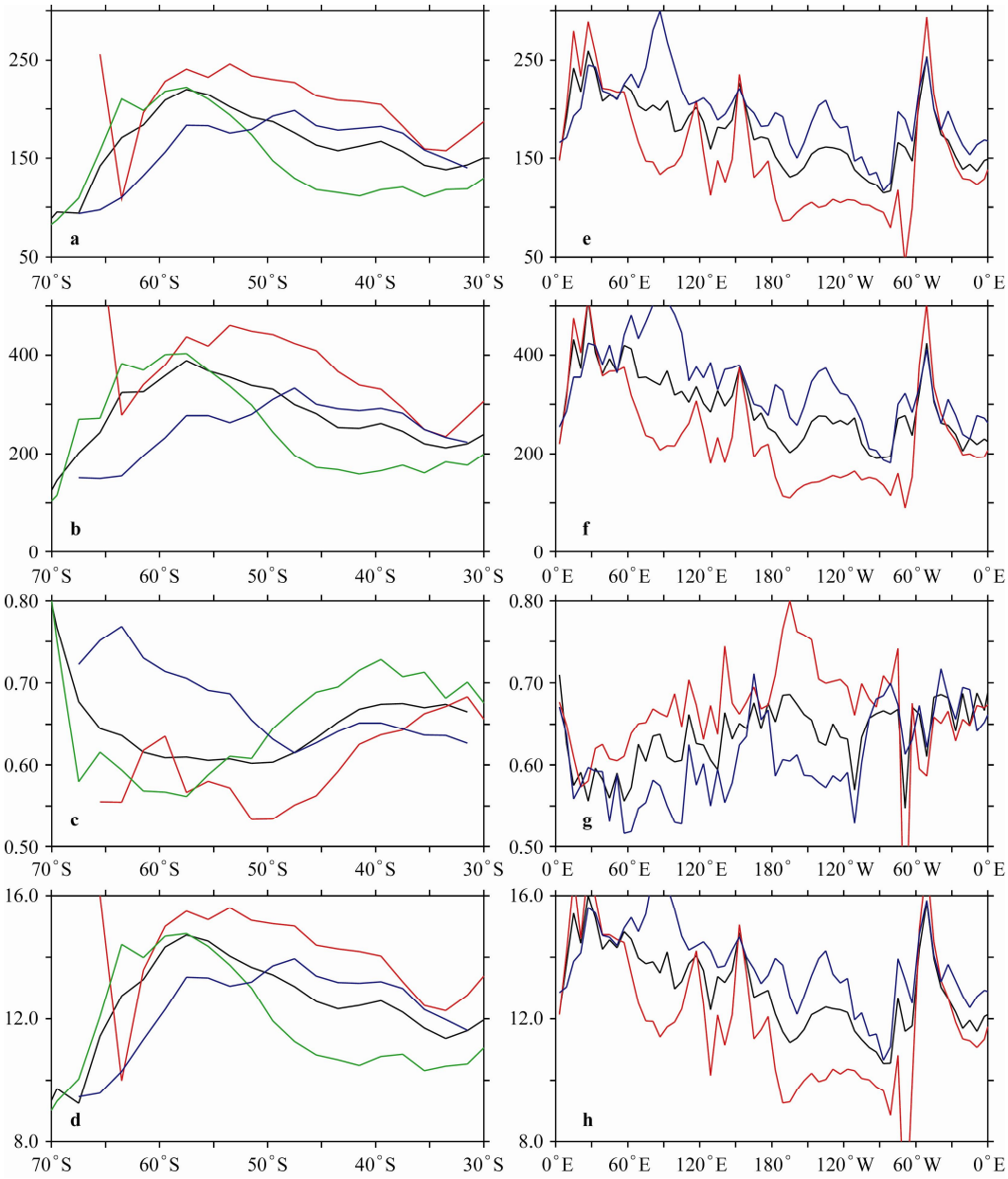

Figure 7 Energy variations of meridional (left panels) and zonal (right panels) sections in the Southern Ocean (unit: $cm^2 \cdot s^{-2}$). **a**, EKE; **b**, MKE; **c**, EKE/MKE; **d**, $\sqrt{EKE}$ (unit: $cm \cdot s^{-1}$. Black lines: mean values of the entire Southern Ocean; red lines: mean values of southern Indian Ocean; green lines: mean values of southern Pacific Ocean; blue lines: mean values of southern Atlantic Ocean). **e**–**f** are the same as **a**–**d** but for zonal sections (black lines: mean values of the entire Southern Ocean; red lines: mean values of the northern part of Southern Ocean 30°S–45°S; blue lines: mean values of the southern part of Southern Ocean 45°S–60°S).

(2) Standard variance ellipses are useful for plotting the variability of both the magnitude and direction of vectors. This indicates that both the Agulhas Return Current and the East Australian Warm Current are stable supplements of the near-surface ACC. During the austral winter, the current velocity increases because of the enhanced westerly wind. Aroused by the meridional motion of the ACC, the meridional velocity shows greater characteristics of instability than the zonal velocity does on the core current. Additionally, the ACC exhibits an eastward declining trend in the core current velocity from southern Africa.

(3) The characteristics of the ACC are discussed from energy perspective. The energy distribution suggests that EKE, MKE, and $\sqrt{EKE}$ are strong over the core currents of the ACC, but that EKE/MKE is the converse; there is much less (more) eddy dissipation in the regions with strong (weak) energy distribution.

(4) Both the meridional and zonal energy variations are studied to illustrate additional details of the energy characteristics of the ACC. Generally, all the energy forms except EKE/MKE present west–east reducing trends, which coincide with the velocity statistics. Eddy dissipation has a

great effect on the MKE in the northern part of the Southern Ocean.

Acknowledgments This work was supported by the National Natural Science Foundation of China(Grant no. 41306206), the Basic Scientific Fund for National Public Research Institutes of China, Chinese Polar Environment Comprehensive Investigation & Assessment Programmes (Grant nos. CHINARE2013-01-01, CHINARE2013-04-01), Projects IC2010011, A908-JK1006, and JDKC01-02 supported by the Chinese Arctic and Antarctic Administration, SOA, and the Ministry of Science and Technology of China (Grant no. 2010CB950301).

References

1 Ryan S, Melicie D, Sean W, et al. The Antarctic CP Current, Ocean Surface Currents, 2000, http://oceancurrents.rsmas.miami.edu/southern/antarctic-cp.html.

2 Gordon A L, Taylor H W, Georgi D T. Antarctic oceanographic zonation// Dunbar M J. Polar Oceans: Proceedings of the Polar Oceans Conference. Arctic Institute of North America, 1977: 44-76.

3 Sokolov S, Rintoul S R. Multiple jets of the Antarctic Circumpolar Current south of Australia. J Phys Oceano, 2007, 37(5): 1394-1412, doi: 10.1175/JPO3111.1.

4 Piola A, Figueroa H A, Bianchi A. Some aspects of the surface circulation south of 20°S revealed by first GARP Global Experiment Drifters. J Geophys Res, 1987, 92(C5): 5101-5114, doi: 10.1029/JC092iC05p05101.

5 Wilkin J L, Morrow R A. Eddy kinetic energy and momentum flux in the Southern Ocean: Comparison of a global eddy-resolving model with altimeter, drifter, and current-meter data. J Geophys Res, 1994, 99(C4): 7903-7916.

6 Rintoul S R, Sokolov S. Baroclinic transport variability of the Antarctic Circumpolar Current south of Australia (WOCE repeat section SR3). J Geophys Res, 2001, 106(C2): 2815-2832.

7 Assireu A T, Stevenson M R, Stech J L. Surface circulation and kinetic energy in the SW Atlantic obtained by drifters. Cont Shelf Res, 2003, 23(2): 145-157, doi: 10.1016/S0278-4343(02)00190-5.

8 Oliveira L R, Piola A R, Mata M M, et al. Brazil current surface circulation and energetics observed from drifting buoys. J Geophys Res, 2009, 114(C1), doi: 10.1029/2008JC004900.

9 Niiler P P. The world ocean surface circulation // Church J, Siedler G, Gould J. Ocean circulation and climate-observing and modeling the global Ocean. London: Academic Press, 2001: 193-204.

10 Hansen D V, Poulain P M. Quality control and interpolations of WOCE-TOGA drifter data. J Atmos Oceanic Technol, 1996, 13(4): 900-909.

11 Kummerow C, William B, Toshiaki K, et al. The Tropical Rainfall Measuring Mission (TRMM) sensor package. J Atmos Oceanic Technol, 1998, 15(3): 809-817.

12 Maximenko N A, Niiler P P. Hybrid decade-mean global sea level with mesoscale resolution // Saxena N K. Recent Advances in Marine Science and Technology 2004. Honolulu, Hawaii: PACON Int., 2005: 55-59.

13 Centurioni L R, Niiler P P. Observations of inflow of Philippine sea surface water into the South China Sea through the Luzon Strait. J Phys Oceanogr, 2004, 34(1): 113-121.

14 Gao L B, Yu W D. Observations and analysis on seasonal variation of western boundary currents and eddy structures in the western Pacific Ocean of the low latitudes. Adv Marine Sci, 2008, 26(3): 317-325.

15 Orsi A, Whitworth III T, Nowlin Jr W D. On the meridional extent and fronts of the Antarctic Circumpolar Current. Deep Sea Res, 1995, 42(5): 641-673.

16 Nishida H, White W B. Horizontal eddy fluxes of momentum and kinetic energy in the near-surface of the Kuroshio Extension. J Phys Oceanogr, 1982, 12(2): 160-170.

17 Legeckis R, Gordon A L. Satellite observations of the Brazil and Falkland Currents-1975-1976 and 1978. Deep Sea Res, 1982, 29(3): 375-401, doi: 10.1016/0198-0149(82)90101-7.

18 Chelton D B, Schlax M G, Witter D L, et al. Geosat altimeter observations of the surface circulation of the Southern Ocean. J Geophys Res, 1990, 95(C10): 17877-17903, doi: 10.1029/JC095iC10p17877.

19 Kundu P, Cohen I. Fluid mechanics(2nd edn) San Diego, Calif: Academic Press, 1990: 730.

20 Patterson S L. Surface circulation and kinetic energy distributions in the Southern Hemisphere oceans from FGGE drifting buoys. J Geophys Res, 1985, 15(7): 865-883.

21 Bryden H L. Sources of eddy energy in the Gulf-Stream recirculation region. J Marine Res, 1982, 40(4): 1047-1068.